Limnol. Oceanogr., 41(7), 1996, 1404–1414

A preliminary study of the geochemical and microbiological characteristics of modern sedimentary concretions

W. M. Duan
Postgraduate Research Institute for Sedimentology, University of Reading, Reading RG6 6AB, U.K.

D. B. Hedrick
Center for Environmental Biotechnology, University of Tennessee, Knoxville 37932

K. Pye and M. L. Coleman
Postgraduate Research Institute for Sedimentology, University of Reading

D. C. White
Environmental Science Division, Oak Ridge National Laboratory, Oak Ridge, Tennessee 37831, and
Center for Environmental Biotechnology, University of Tennessee

Abstract

Parallel mineralogical, geochemical, and lipid biomarker analyses of sedimentary siderite concretions and their host sediments were undertaken to give detailed information about the microbially mediated diagenetic processes involved. Concretions were collected from two contrasting environments at Warham, north Norfolk—typical brownish silty marsh sediment and black anaerobic mud from a creek bank—but no major differences in their mineralogy or geochemistry were found. Samples consisted of siderite, amorphous iron oxides, and iron sulfides with more carbonate present in the outer than in the inner parts. Subsamples from the concretions were found to be more similar to each other in their sulfide and organic carbon contents than to the host sediments. The microbiological characteristics revealed by lipid biomarker analysis showed considerable variation between concretions and host sediments, between individual concretions, and between inner and outer parts of the concretions. The predominant sulfate-reducing bacteria were more numerous in the concretions than in host sediments, but varied greatly within the concretions. The biomarker i17:1ω7c for *Desulfovibrio* was enriched within the concretions, suggesting that these bacteria, which are capable of reducing iron directly, played an important role in concretion formation. The lipid biomarker data indicated that the bacterial community changed during concretion formation and that different conditions for preservation existed in the concretions compared with the host sediments.

Sulfur, iron, and organic carbon are the most active components during the early diagenesis of marine sediments (Berner 1985; Canfield and Raiswell 1991; Froelich et al. 1979). Upon exhaustion of the diffusion-limited supply of oxygen, sulfate is microbially reduced to sulfide and ferric iron is reduced to ferrous iron with the concomitant production of bicarbonate (Coleman 1985; Curtis 1983; Lovley et al. 1993). This process results in the formation of authigenic minerals dispersed within the sediment or, in favorable circumstances, concentrated within concretions. In modern salt-marsh environments, diagenetic processes are highly active because of the high production of organic matter and regular inundation by tidal waters (Howarth 1993).

Both geochemical and biological investigations have been carried out intensively, but often separately, in such natural laboratories (King et al. 1985; Jørgensen and Bak 1991; Peterson and Howarth 1987). However, the presence of authigenic carbonate concretions, which are a product of the microbial activity and geochemical reactions in modern salt-marsh environments, has rarely been reported. An exception is the siderite-rich concretions that are actively forming in salt marshes on the north Norfolk coast of England (Pye 1984; Pye et al. 1990).

On the basis of previous work, it is thought that the concretion formation begins with organic degradation mediated by anaerobic microorganisms and the consequent production of available Fe^{2+}, HS^-, and HCO_3^-. Because inorganic iron reduction by H_2S will only produce iron sulfide, which is more stable than iron carbonate, iron sulfide and siderite do not commonly co-occur in the early stages of diagenesis (Curtis 1983). Thus, the unusual association of these minerals in the north Norfolk concretion assemblage may imply direct reduction of Fe^{3+} by microbial activity, rather than indirectly by sulfate reduction (Coleman et al. 1993) and subsequent trapping of HCO_3^- within the concretions. Because the concretions are still forming, they offer us an opportunity to

Acknowledgments

This research was supported by grants GR3/9180 and G3/8131A from the U.K. Natural Environment Research Council to M.L.C. and K.P.

We thank D. Ringelberg for helpful discussions. Critical reviews from Kevin Taylor and an anonymous reviewer and constructive comments from B. P. Boudreau are highly appreciated.

This paper represents University of Reading PRIS contribution 503.

understand the detailed interactions between microbial processes and their inorganic products.

In recent decades, the technique of signature lipid biomarker analysis has been developed to provide quantitative definition of the in situ viable biomass, community structure, and nutritional status of the sedimentary microbiota (White et al. 1979; White 1993). The technique is based on the assumption that all microorganisms contain cell membranes composed of phospholipids and that the fatty acids associated with these lipids can be quantitatively isolated and extracted, thus providing information about viable biomass, microbial community structure, and nutritional stress status. We present results of a preliminary study in which mineralogical, geochemical, and microbial biomarker techniques were used to extend early investigations (Coleman et al. 1993) on the relationships between microbial activity and concretion formation in the north Norfolk salt-marsh system.

Geological background and analytical techniques

Study area—The study area is located at Warham on the coast of north Norfolk, U.K. (Fig. 1). The Warham salt marshes consist of two major geomorphological units: the upper marsh, which was initiated in the mid-Holocene and which in recent decades has accreted steadily in line with sea-level rise in the area (~1 mm yr^{-1}); and the lower marsh, which was formed mainly within the last 50 yr and which has experienced relatively rapid vertical accretion (>1 cm yr^{-1}) (Funnell and Pearson 1989; Pye 1992; Pye et al. 1997). A low aeolian sand ridge separates the two units. The average elevation of the upper marsh is 2.7–2.9 m and that of the lower marsh is 2.0–2.3 m ordnance datum. The groundwater table lies 1.8–2.0 m below the surface of the upper marsh and at depth of 1.0–1.2 m in the lower marsh. The lower marsh is covered by ~30% of tides, whereas the upper marsh is covered only by the highest spring tides (~6% of all tides).

Generally, the upper marsh sediments consist of grayish brown clayey silts; the lower marsh sediments consist of clayey silts, silty sand, and medium sand from the surface downward. A system of tidal creeks is developed on both the upper and the lower marshes. Within the creeks, anoxic black mud commonly occurs on the banks. The surficial 1–2 cm is often oxidized with numerous megafaunal burrows. Below this surface lies 20–50 cm of massive, soft, black, muddy sediment. In the lower marsh, black sandy sediments occur adjacent to the water table. In situ concretions occur most commonly within black sediments (Pye et al. 1990). Although the mineralogy and inorganic geochemistry of the concretions have been investigated in some detail (Pye 1984; Pye et al. 1990; Allison and Pye 1994), little attention has been given to the microbial populations within the concretions and host sediments. To provide more information about these populations, concretions were collected for analysis from three sites, one from the upper marsh and two from the lower marsh.

The sampling site on the upper marsh (UMP) was located in a small creek that leads to the main Stonemeal Creek (Fig. 1). The creekbank sediment at the sampling site consisted of black anaerobic mud with a strong sulfide smell. The upper marsh concretion (UC) was collected from a depth of ~25 cm in the creekbank mud. The lower marsh site (LMP) was a pit dug in the marsh ~20 m away from the nearest creek. The top 25 cm of sediment consisted of dark gray-brown clayey silts with plentiful plant roots. From 25 to 80 cm, the sediment consisted mainly of brownish muddy sand that became slightly sandier with depth. The lower marsh concretion (LC) was found at 25-cm depth in the dark brownish muddy sediments. Sediment samples LM25, which surrounded the concretion, and LM75, from 75-cm depth, were collected from the profile with a spatula. Site LKP was located in a creek in the lower marsh. Two concretions and an adjacent sediment sample were collected at a depth of 15 cm.

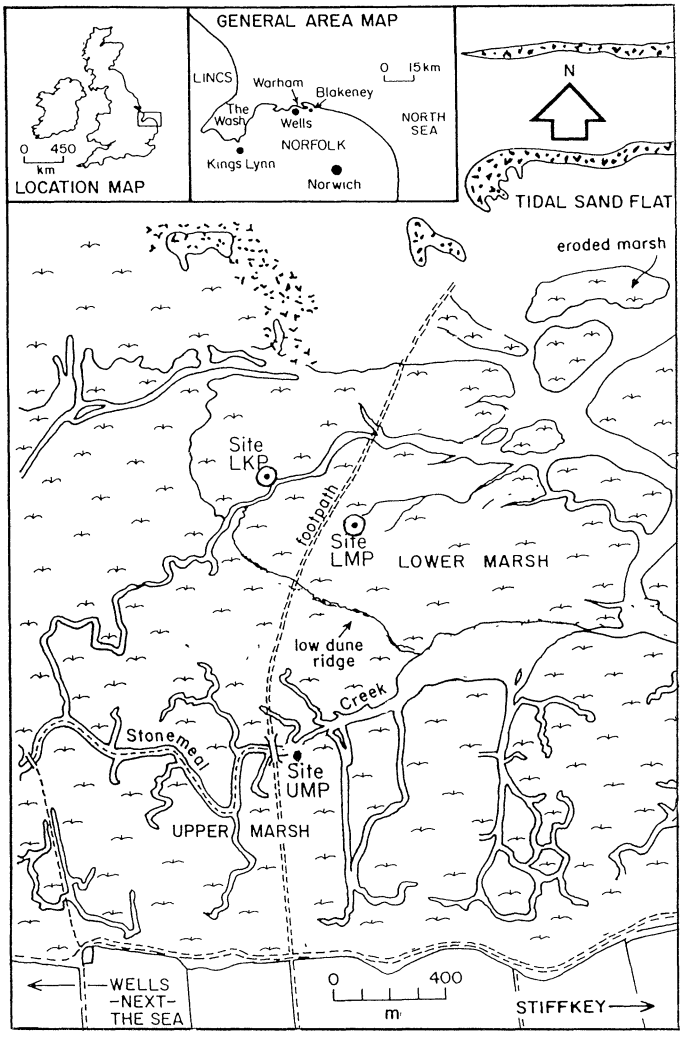

Fig. 1. Location of the study area and sampling sites.

The concretions were preserved in the host sediment at the time of collection. All samples were sealed in plastic bags, transported to the laboratory in dry ice, and stored in a freezer until analysis. Sediment samples were treated in situ by adding zinc acetate to fix the easily oxidizable

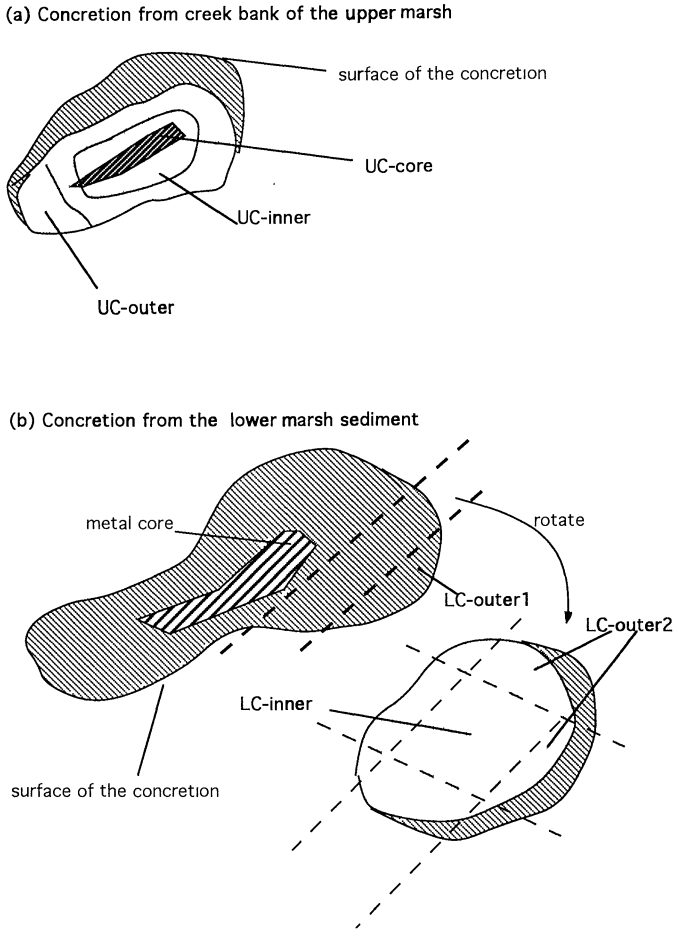

Fig. 2. Diagram of the analyzed concretions showing the individual subsamples. [a.] Concretion from the upper marsh. UC-outer was cut from one end of the concretion, UC-inner was taken from the sides between the outer surface and the core, and UC-core represented the corroded metal core. [b.] Concretion from the lower marsh. LC-outer1 was sawn off the larger end, parallel to the long axis of the concretion. A central slice was obtained by making a second cut parallel to the first. LC-outer2 was obtained from the outer part of the central slice by making four additional chisel cuts; LC-inner was the inner part of the central slice adjacent to LC-outer2. (The noncorroded metal core next to LC-inner was not taken.)

sulfide. When we returned to the laboratory, the concretions were cut while still frozen and divided into subsamples with a chisel. After the subsamples were freeze-dried and ground, they were split for geochemical, mineralogical, and microbial lipid analyses.

Figure 2 shows schematically how the concretions were divided into subsamples and conceptualized as being adjacent to the core, interior, or adjacent to the surface. This scheme represents a great simplification given the lack of mineralogical and textural uniformity observed in the concretions. Concretions were hard, dense, cemented areas interspersed with friable and chalky material. The oxidized surface varied from white, brown, purple, to black (in the fresh state, concretions are uniformly black). Sample size requirements for different analyses determined how small a volume could be sampled.

Table 1. Summary of the subsamples analyzed in this investigation: U—upper marsh; L—lower marsh; M—host mud or sediment; C—concretion; K—a creek in the lower marsh; A and B—concretions from the same site.

UM	Creek mud from the upper marsh (site UMP) adjacent to concretion UC
UC	Concretion from site UMP. Subsamples include
UC-outer	One end of the concretion, outer and some interior material, not adjacent to the core
UC-inner	Mainly interior material adjacent to the core
UC-core	Corroded metal core of the concretion
LM25	Sediment from the lower marsh (site LMP), 25-cm depth, fine gray, adjacent to concretion LC
LM75	Sediment from site LMP, 75-cm depth, gray sandy sediment, near groundwater table
LC	Concretion from site LMP. Subsamples include
LC-outer1	Material mostly adjacent to the surface of the concretion
LC-outer2	Outer part adjacent to subsample LC-inner
LC-inner	Material from the interior adjacent to the metal core
KM	Sediment from a creekbed in the lower marsh (site LKP)
KCA and B	Concretions A and B adjacent to the sediment KM
KCA-outer	Mainly outer part of the concretion
KCA-inner	Mainly interior material
KCB-outer	Mainly outer part of the concretion
KCB-inner	Mainly interior material

UC (Fig. 2a) was an ellipsoid (5 × 8 cm) that contained a corroded metallic nucleus. Corrosion of the metal core in UC was so advanced that it had taken on the appearance of rotten wood. LC was a prolate ellipsoid with one end larger than the other (8–12 × 30 cm). Two outer subsamples (LC-outer1 and LC-outer2) and one inner subsample (LC-inner) were obtained from the larger end of the concretion (Fig. 2b). Two additional concretions (KCA and KCB) collected from site LKP were subdivided similarly, but subsamples were obtained only from the inner and outer parts of the concretions. The full list of subsamples is summarized in Table 1.

Analytical methods—Geochemical analyses included determinations of reduced sulfur, total and reactive iron, and organic and inorganic carbon. Mineralogical composition was determined by X-ray powder diffraction (XRD). Reduced sulfur was determined by means of the method of Canfield et al. (1986), but with modifications to the reaction vessel and the flushing and trapping tube apparatus. The black host mud was treated in the field with zinc acetate to fix acid-volatile sulfide (AVS), but concretions were not so treated. Controlled tests with and without zinc acetate showed that most of the elemental sulfur in untreated samples resulted from the oxidation

of AVS after sampling, even when the samples were freeze-dried. Because concretions were not treated with zinc acetate, which resulted in oxidation of sulfide to elemental sulfur, this proportion was attributed to AVS based on separate experimental data (Duan et al. unpubl.).

AVS was extracted with 40 ml of 6 N HCl for 1 h at room temperature in a round-bottom flask. The H_2S gas that was generated was trapped in a copper(II) chloride solution (25 ml, 0.1 M), and the amount of sulfide was determined by titrating the solution with EDTA against a standard. Pyrite sulfur was digested as H_2S by further boiling the sample in 6 N HCl and chromium chloride solution for 90 min; the sulfide was trapped separately and quantified, as for AVS. Total iron was determined by X-ray fluorescence spectrometry (XRF). HCl-extractable iron (Leventhal and Taylor 1990) was digested by shaking samples in 20 ml of 6 N HCl for 2 h and determined by inductively coupled plasma spectrometry (ARL35000 instr.). Organic carbon was determined by a modified Walkley-Black method (Gaudette et al. 1974). Carbonate carbon was determined by digesting the samples in 4 N HCl in a calcimeter. The volume of CO_2 generated from the reaction was recorded after the reaction ceased, and the carbonate carbon content was calculated against a standard of pure $CaCO_3$.

Phospholipids were extracted with a single-phase chloroform-methanol-water extraction method (Bligh and Dyer 1959). Lyophilized material was combined with 37.5 ml of chloroform, 75 ml of methanol, and 30 ml of phosphate buffer (0.5 mM, pH = 7.2), agitated, and allowed to extract for 2 h. The mixture was centrifuged and the mixed organic and aqueous phase was decanted into a separatory funnel. The delipidated solids were reserved for further analysis. Additional 37.5-ml volumes of both chloroform and water were then added to the extract and mixed, and the aqueous and organic phases were allowed to separate overnight. The lower organic phase was drained through filter paper, and the solvent was removed by means of a rotary evaporator with 37°C water bath to yield the total lipid extract.

The total lipid was fractionated into neutral lipid, glycolipid, and polar lipid fractions by silicic acid column chromatography (White et al. 1983). The polar lipid fraction was treated with a mild alkaline methanolysis to liberate the polar lipid (phospholipid) fatty acids (PLFA) as their methyl esters (White 1968). PLFA methyl esters were quantified by capillary gas chromatography (Shimadzu GC-9A instr.) with a 50-m HP-1 capillary column under a temperature program of 100°C for 1 min, 10°C min^{-1} to 150°C, hold for 1 min, 3°C min^{-1} to 282°C, and hold for 5 min (Vestal and White 1989). Preliminary peak identification was by equivalent chain length calculations based on synthetic standards and a bacterial fatty acid mix. Peak identifications were verified by gas chromatography-mass spectroscopy with the same column and temperature program on an HP 5890 Series II.

Residue fatty acids (ResFA) were released from the delipidated solids with a strong acid methanolysis (Hedrick et al. 1991). Solids were suspended in 10 : 1 : 1 methanol : chloroform : concentrated HCl in a sealed 50-ml test tube, heated at 100°C for 1 h, cooled, and extracted 3 times with hexane. After the solvent had been removed from the pooled extracts, the hydroxy fatty acid methyl esters were derivatized with BSTFA (Pierce) and analyzed as for PLFA. Because of the possible high input of terrigenous nonhydroxylated and 2-hydroxylated fatty acids, only the more reliable bacterial 3-hydroxy fatty acids are reported.

The fatty acid nomenclature is as follows: the number of carbons, a colon, the number of unsaturations, an ω, and then the distance of the unsaturation from the methyl end of the fatty acid. The prefix "i" stands for *iso*-branched, "a" for *anteiso*-branched, "10Me" for a methyl group 10 carbons from the carboxylate end of the molecule, "br" for a methyl group of unknown position, "poly" for a polyenoic of unknown number and position, and "cy" for cyclopropyl moiety. The suffix "c" stands for the *cis* isomer of a monounsaturated fatty acid, "t" for the *trans* isomer, and "a" and "b" for the first and second fatty acids eluting with indistinguishable names. For example, 16:0 is hexadecanoic acid in the IUPAC nomenclature, and 18:1ω7c is *cis*-octadec-11-enoic acid.

Results

Mineralogy and geochemistry—When concretions were exposed to air, parts of the surface changed from black to brownish red. The texture and mineral composition were quite heterogeneous, ranging from very dense and hard or fragile to soft and clayey. The differences in color and texture indicate variations in the distribution of reactive components and authigenic precipitates during concretion formation. The mineral assemblage and microbial activities in each color zone are expected to be significantly different. However, because of limitations on the required subsample size and the fact that the concretions were wholly black when fresh, the subsamples were significantly heterogeneous in texture and composition. The mineralogical features determined by XRD showed that siderite and magnesian calcite are the major authigenic cement phases in the concretions, although authigenic iron sulfide and aragonite are also locally significant. The concentration of authigenic carbonates (mainly siderite) ranged up to 15–30 wt% of the total crystalline minerals according to the semiquantitative XRD analysis and previous determination by microprobe analysis (Pye 1984). The carbonate cements were slightly more abundant in the outer subsamples. More magnesian calcite and aragonite were also found in the outer than in the inner subsamples. Pyrite and crystalline iron monosulfides, such as mackinawite and greigite, were not detected by XRD.

Scanning electron microscopy (SEM) examination of the morphology of the cement phases in the concretions revealed that authigenic siderite and calcite were closely intergrown and that siderite occurred in different habits, including pseudo-cubic, rhombohedral, and acicular. Magnesian calcite occurred mainly as aggregations of rhombic and acicular crystals. Some Fe-S phases were detected by SEM and were shown to occur as irregular plates, sheets, or needle clusters. The host sediment was

Table 2. Geochemical composition of marsh sediments and concretions (in wt% of dry sediment; nd—not determined).

Sample	Total Fe	React. Fe	AVS Fe	Pyrite-Fe	Org C	Inorg C	Total RS	AVS	PyS
UM	4.70	3.70	0.642	0.057	2.54	0.27	0.866	0.735	0.131
UC-outer	18.35	18.04	0.698	0.135	1.34	1.74	1.108	0.799	0.309
UC-inner	11.24	11.10	0.769	0.149	1.16	1.69	1.222	0.880	0.342
UC-core	42.29	41.45	nd	nd	nd	nd	nd	nd	nd
LC-outer1	13.30	13.67	0.823	0.094	1.32	1.39	1.157	0.942	0.215
LC-outer2	13.40	13.00	0.736	0.174	1.27	0.80	1.241	0.843	0.398
LC-inner	13.60	12.70	0.623	0.127	1.16	0.53	1.003	0.713	0.290
LM25	2.40	1.13	0.024	0.000	0.38	0.03	0.028	0.027	0.001
LM75	2.30	0.49	0.011	0.052	0.57	0.12	0.133	0.013	0.120
KCA-outer	15.53	14.62	0.693	0.188	1.57	2.24	1.225	0.794	0.431
KCA-inner	21.49	20.86	0.514	0.110	1.26	0.39	0.841	0.589	0.252
KCB-outer	15.41	15.24	0.901	0.170	1.92	3.11	1.422	1.032	0.390
KCB-inner	20.20	18.98	0.861	0.235	1.83	1.31	1.524	0.986	0.538
KM	1.74	0.94	0.216	0.066	1.88	0.43	0.398	0.284	0.114

mainly composed of detrital minerals—quartz, feldspar, clay minerals, and some carbonate shell fragments. Siderite and iron sulfide phases were not detected by XRD or SEM performed on the host sediments.

The geochemical characteristics of the authigenic components are listed in Table 2. Figure 3 shows the 6 N HCl-extractable iron and total iron contents. The classification of 6 N HCl-extractable iron includes iron derived from AVS, carbonate, and most of the oxyhydroxides. This portion has previously been used as a measure of the reactive component in sedimentary systems (e.g. Postma 1982; Leventhal and Taylor 1990). In the concretions, total iron content ranged from 11 to 21% by dry weight, while the host sediments contained only 2–5% Fe, indicating enrichment of iron in the concretions. Of the total iron in the concretions, >93% was present as extractable iron, whereas in the host sediments, the extractable iron content varied from 21 to 79% of total iron. Total iron in the corroded metal core of subsample UC-core was up to 42%, 98% of which was 6 N HCl extractable.

Total reduced sulfur species in the concretions ranged from 0.8 to 1.5% by dry weight. There was a large variation in the total reduced sulfur (TRS) content of the surrounding sediments. In the black, anaerobic creek sediments, the concentration of TRS ranged from 0.4 to 0.9%, whereas it was only 0.03% (Fig. 4) in the brownish marsh sediments. The enrichment of TRS in the concretions indicated a relative accumulation of sulfide within the concretion compared to the surrounding sediments. Reduced sulfur species were operationally divided into AVS and pyrite sulfur (PyS) (Cornwell and Morse 1987). AVS was the dominant component (60–80%) in the reduced sulfur pool of the concretions, which suggested that the process of pyritization occurred at a very early stage. The increase in PyS in sample LM75 compared with LM25 indicates further pyritization with deeper burial. There was no clear pattern in the variability of TRS, AVS,

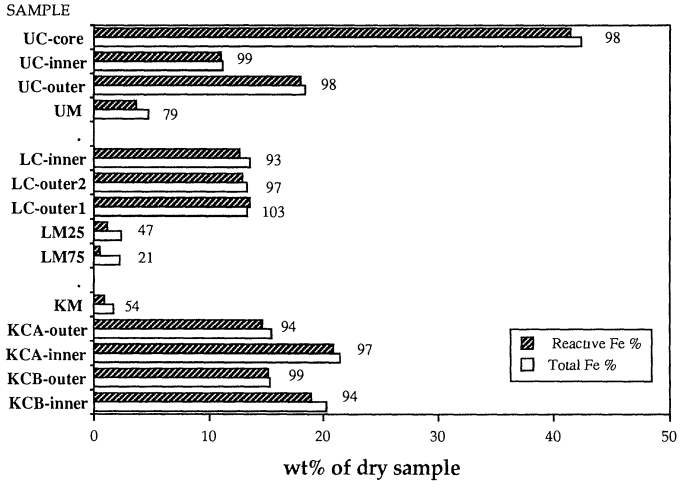

Fig. 3. Total and reactive iron. Total iron was determined by XRF and reactive iron by extraction with 6 N HC. Numerical values indicate reactive iron as a percentage of total iron content.

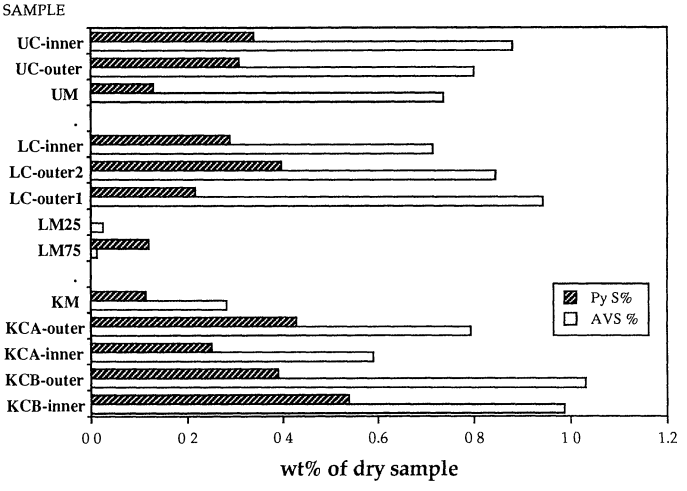

Fig. 4. Acid-volatile sulfur and pyrite sulfur contents of the concretions and their host sediments.

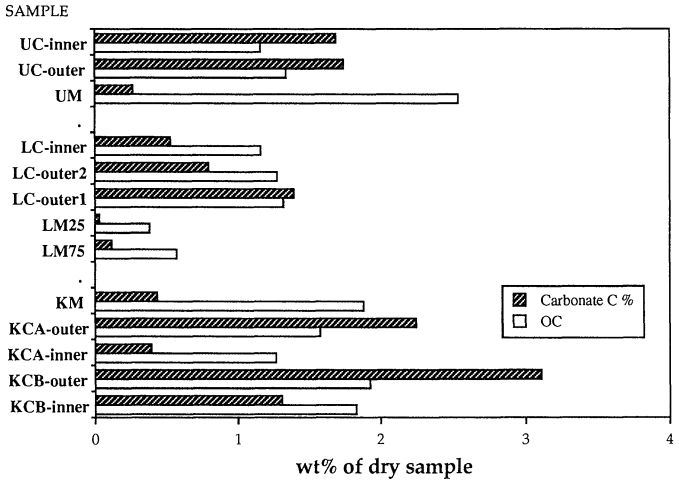

Fig. 5. Organic and inorganic carbon contents in concretions and their host sediments.

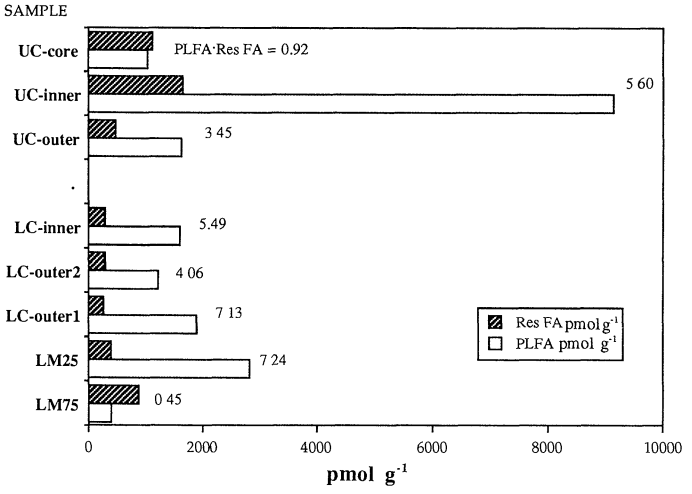

Fig. 6. Polar lipid fatty acid (PLFA) and residue 3-hydroxy-fatty acid (ResFA) contents of the concretions and their host sediments. Full details of the signature lipid data are available from the authors on request.

or PyS between the outer and inner subsamples of the concretions. Two lower marsh concretions (LC and KCA) showed more TRS in the outer rim than in the inner part, whereas two other concretions (UC and KCB) had more TRS inside than in the outer rim. The diversity of reduced sulfur could not be related to concretion structure at this level of analysis.

The concentrations of organic and inorganic carbon in the concretions and their host sediments are presented in Fig. 5. In LC, the organic carbon content was much higher than in its host sediment (LM25). In contrast, the black mud in the lower marsh creek (KM) had about the same level of organic carbon as the concretion contained within it, and the upper marsh creek host mud (UM) had more organic carbon than did its contained concretion. In all the concretion samples analyzed, the contents of carbonate carbon and of organic carbon were slightly higher in the outer than in the inner subsamples.

Lipid biomarker analyses—Eight samples were chosen for lipid biomarker signature analyses. The amounts of PLFA and ResFA are presented as a bar graph in Fig. 6. Total PLFA provided a measure of the viable microbial biomass in the sediment, and the ResFA provided an indicator of the accumulation of dead bacterial cells due to cell turnover. Published values for the ratio of PLFA : ResFA in pure cultures of gram-negative bacteria ranged from 6.7 for *Escherichia coli* (Balkwill et al. 1988) to 7.0 and 11.5 for *Desulfomonile tiedjei* grown under different culture conditions (Edlund et al. 1985) and from 3.7 to 23.8 for six strains of *Desulfovibrio* (Ringelberg et al. 1994). Although the ResFA is a biomarker for the gram-negative bacteria, it is degraded much more slowly than is PLFA, especially in anaerobic sediments (Harvey et al. 1986).

The three subsamples from the lower marsh concretion (LC-outer1, LC-outer2, and LC-inner) had similar amounts of PLFA and ResFA, and had lower biomass per gram dry weight than did the host mud (LM25). The outer part of UC was similar to the lower marsh concretion samples in the pattern of PLFA and ResFA. However, the inner material (UC-inner) from around the core of UC had the highest biomass per gram of any of the samples, and the corroded iron core (UC-core) had the largest accumulation of ResFA of any concretion samples. Therefore, it seemed that the microbial biomass was greatly increased in UC and that the cell turnover was greatly increased within the corroded iron core.

Differences in the species composition of microbial communities are reflected in the pattern of PLFA present. Figure 7 provides a summary of the monounsaturated PLFA, grouped by position of the unsaturation, and the polyenoic PLFA. There was a great difference in the pattern of monounsaturated PLFA in the Lower Marsh concretion and its host mud, with a greatly increased pro-

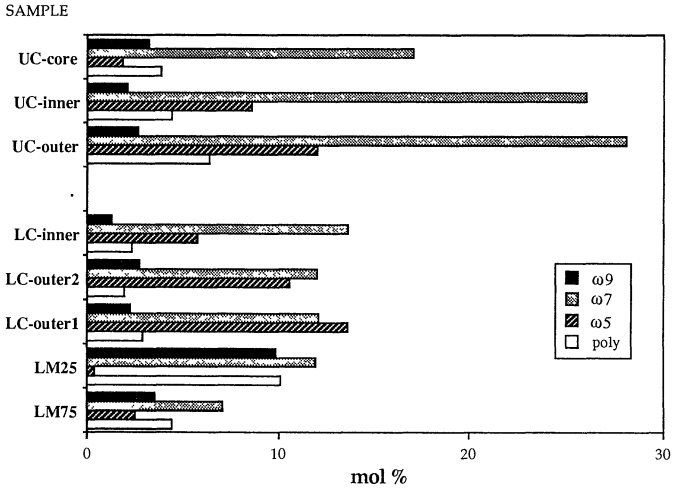

Fig. 7. Selected community structure groups of polar lipid fatty acids. ω9, ω7, ω5—monounsaturated with the distance (C9, C7, C5) from the methyl end of the fatty acid; poly—polyunsaturated.

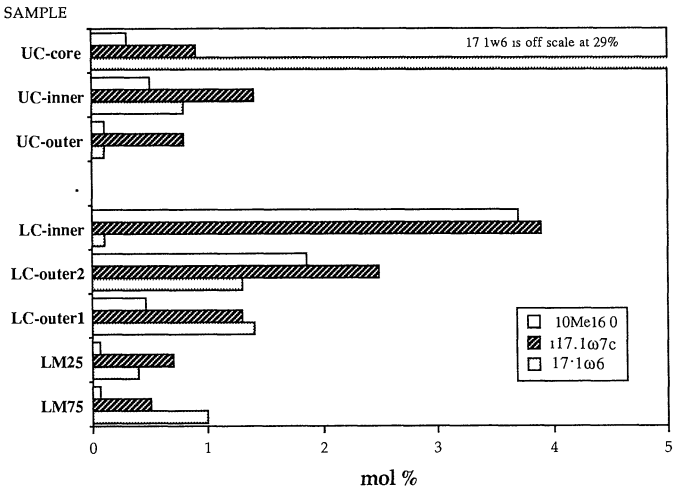

Fig. 8. Polar lipid fatty acid biomarkers for sulfate-reducing bacteria.

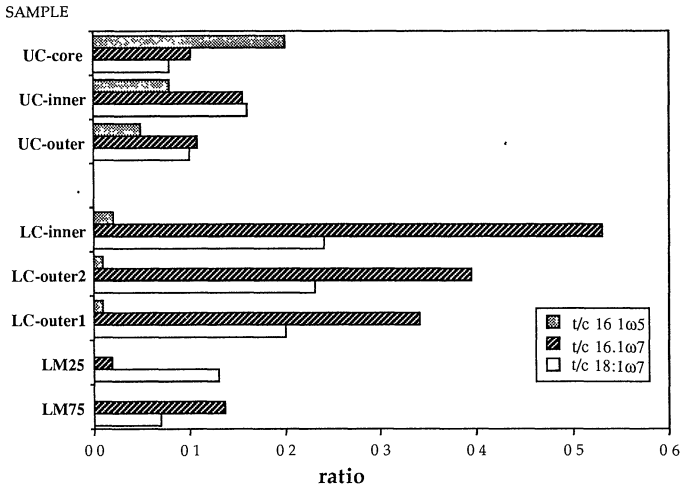

Fig. 10. Metabolic status markers, as molar ratio of a *trans* to the *cis* fatty acid.

portion of ω5 monounsaturates and decreased proportions of ω9 and polyenoics in the concretion. The ω9 PLFAs were produced by some bacteria but were the predominant monounsaturates in eucaryotes, and the polyenoics were indicative of eucaryotic biomass. The spatial variation of ω9 indicated that as the concretion grew by cementing sediment particles, eucaryotes were mostly excluded from the occupied pore volume.

Examining a particular PLFA known to be in specific members of the community is another approach to assessing changes in microbial community composition. The sulfate-reducing bacteria (SRB) are an important part of the microbial community of marine sediments (Skyring 1987). Figure 8 shows the species distribution of some distinctive signature biomarkers from PLFA for SRB (Taylor and Parkes 1983; Dowling et al. 1986). The 10Me16:0 in the midchain branched saturated structure group is an indicator for *Desulfobacter*. *Desulfovibrio*s have significant i17:1ω7c in the unsaturated branched monoenoic group, and 17:1ω6 is specific for *Desulfobulbus*. All three biomarkers were enriched in the lower marsh concretion compared with its host mud, with 17:1ω6 greater in the outside and i17:1ω7c and 10Me16:0 greater in the inside of the concretion. UC exhibited a very different pattern from LC, with the biomarkers suggesting SRB in subsamples UC-outer and UC-inner and a very large increase in 17:1ω6 in UC-core.

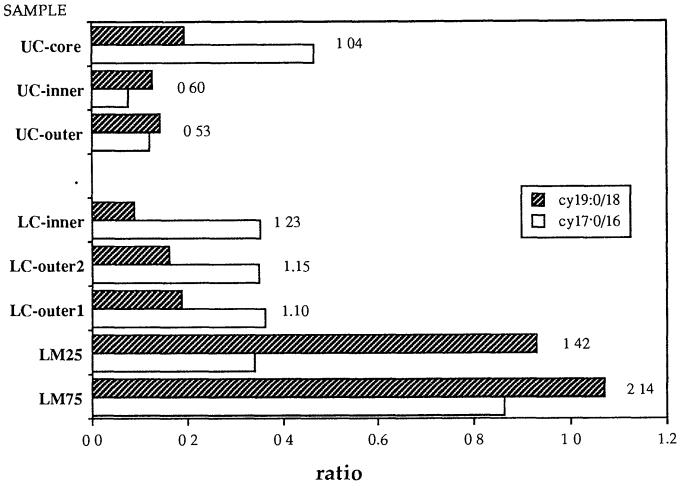

Fig. 9. Metabolic status markers, as the molar ratio of a cyclopropyl to the *cis* fatty acid. The sums of all stress markers (cy : *cis* and *trans* : *cis*) are indicated as numerical values.

The metabolic status markers shown in Figs. 9 and 10 are ratios of a fatty acid characteristic of starving or stressed bacteria to the metabolic precursor of that fatty acid. *Trans*-monounsaturated PLFA and cyclopropyl PLFA are formed from their precursor *cis* isomers of the monounsaturates. The sediment samples LM25 and LM75 were distinguished from the concretions by high ratios of the cyclopropyl stress markers. The ratio cy17:0 : 16:1ω7c, an indication of starvation, showed twice as much stress in LM75 as found in LM25. LC was distinguished by much higher levels of *trans* : *cis* 16:1ω7 and higher levels of *trans* : *cis* 18:1ω7 than found in the other samples, and its subsamples (LC-outer1, LC-outer2, and LC-inner) were similar to each other in the pattern of the metabolic stress marker profiles. In UC-outer and UC-inner, the overall *trans* : *cis* ratios were lower than they were in LC except for *trans* : *cis* 16:1ω5, which was many times more concentrated than in the other samples. Additionally, UC-core had >3 times the level of cy17:0 : 16:1ω7c than the other two samples from that concretion. UC-core also had the highest cy17:0 : 16:1ω7c of all samples analyzed.

Discussion

Characteristics of the host sediments—The above results show clear geochemical differences between the typical marsh sediments and those from the creekbanks. The higher levels of organic carbon and iron sulfides in the black creek sediments of both the upper and lower marsh are due partly to the active worm fauna and partly to a

regular supply of fresh organic nutrients from the tidal creek system. When geochemical features of lower marsh sediments at 25- and 75-cm depths were compared (Table 2), the deeper sample had a lower percentage of reactive iron and its sulfide minerals were more pyritized. The abundant AVS relative to PyS indicates that pyritization is at a very early stage in this salt-marsh environment. The correlation of organic carbon, sulfides, and reactive Fe in the sediments is in accordance with the diagenetic pattern observed in fully marine environments (Berner 1985).

The signature lipid biomarker analysis on the lower marsh sediment profile (Fig. 6) showed that the viable biomass, indicated by the total PLFA, decreased with depth. PLFA decreased when the organic carbon deposited in the sediment was degraded and access to electron acceptors was restricted (Findlay and Dobbs 1993; Parkes and Taylor 1983; Rodier and Khalil 1982). There was a greater accumulation of dead biomass (as indicated by ResFA) in the deeper parts of the sediments (LM75) than in the shallow sample owing to cell death by starvation and very slow biodegradation of the ResFA relative to PLFA. The nutritional status of bacteria was also more stressed in the deeper part of the profile, as indicated by a higher ratio of stress marker (cyclopropyl : *cis* monounsaturates) in LM75 (Fig. 9). Microbial biomarkers in salt-marsh sediments have rarely been examined as deep as 25 or 75 cm because most biological activity occurs at much shallower depths; nevertheless, PLFA profiles in the sediment samples from this study were similar to those of Volkman et al. (1980).

Comparison of host sediments and concretions—Concretions were distinguished geochemically from their host sediments by their much higher total iron contents, their uniformly high proportion of reactive iron, and their higher total reduced sulfur (Figs. 3, 4). However, the proportion of sulfide-bonded iron (AVS + PyS) constituted only a minor fraction (2–8%) of reactive iron in concretions. Moreover, there was a large proportion of 6 N HCl-extractable Fe that could not be accounted for by siderite-bonded Fe, even assuming that the total inorganic carbon was present as siderite. XRD showed no crystalline Fe oxides in the concretions; thus, the surplus extractable Fe may be in the form of amorphous Fe oxides. This evidence indicated that although SRB were active within concretions, the microbial metabolism took place in an Fe-rich anaerobic microenvironment. The induced diagenetic reactions would involve the production and trapping of bicarbonate and precipitation of siderite and Fe oxides, but with relatively little production of iron sulfides.

The signature lipid biomarker analysis indicates that although the total PLFA and ResFA contents of the three concretion subsamples in the lower marsh were similar to those of their host mud (Fig. 6), the component PLFA were very different. The typical eucaryote PLFA ω9 monounsaturates and polyenoics were greater in the host sediment than in its concretion (Fig. 7). The much reduced eucaryote biomass in the concretion relative to its host sediment was most likely due to the radically reduced porosity of the concretion, which led to physical exclusion of eucaryotes. The increase of ω5 PLFA in the concretions probably resulted from a shift in the bacterial population that made up the microbial community in the concretion. The distribution pattern of ω5 and other PLFA data (Figs. 8–10) clearly indicated a very different viable microbial community within the concretion from that in its host sediment, without greatly increasing the viable biomass in the concretion.

Because the ResFA had not accumulated in the concretion and there was no increased turnover of cells, the bacterial communities of both sediment and concretion seemed stressed to about the same degree. Nevertheless, the microbial community in the concretion had a different pattern of metabolic stress markers from those in the host sediment. Because *trans*-monounsaturated and cyclopropyl PLFA were formed from the precursor *cis* isomers of the monounsaturates under metabolic stress, the ratios of *trans* : *cis* and cy : *cis* are indications of the degree of metabolic stress, which in turn was related to the access to nutrients (Guckert et al. 1986; White et al. 1979; White 1993). The most remarkable distinction in metabolic status between LC and its host sediment was the high *trans* : *cis* ratios, especially *trans* : *cis* 16:1ω7 and 18:1ω7, in the concretion and the high level of cyclopropyl stress markers in its host sediment (Figs. 9, 10). The stress biomarkers indicated that within the concretion, microorganisms survived by adjusting or producing even more *trans*-monounsaturated 16:1ω7 and 18:1ω7 to cope with the stressed condition. The SRB biomarkers (Fig. 8) showed that there were more SRB in the concretion, especially in the inner part, than in the host sediment. The increase in SRB *Desulfovibrio*, as shown by a high level of the biomarker i17:1ω7c within the concretion, may imply a shift from reducing SO_4 to directly reducing ferric Fe in order to cope with the particular diagenetic environment within the concretion (Coleman et al. 1993).

Microbial metabolism within concretions—Because concretions grow by cementing together sediment particles, any microbiological or geochemical differences related to concretion growth should be found on a transect from the center of the concretion out into the host sediment. However, because of the sampling constraint, the concretions investigated here were simply divided into subsamples that contained either more surface material, more interior material, or the Fe core. Thus, the available microbial comparisons at this stage were limited to the subsamples from the outer and inner parts of LC and to the metal core vs. the main body of UC.

Overall, the microbial community in LC was more homogeneous across the three subsamples and was significantly different from UC. LC was characterized by a higher proportion of the SRB biomarkers i17:1ω7c for *Desulfovibrio* and 10Me16:0 for *Desulfobacter* (Fig. 8) and a high *trans* :*cis* ratio of the stress indicator 16:1ω7 in the body of the concretion (Fig. 10). The UC, on the other hand, had the highest PLFA content in UC-inner (by a factor of 3), indicating a process at that location that

supported a higher viable biomass. The microbial community structures within UC had much more ω7 monounsaturated PLFA and a somewhat lower proportion of SRB. Also, the sum of the metabolic stress biomarkers was lowest in the body of UC, whereas the corroded core showed the same degree of stress as the lower marsh mud and concretion samples (Fig. 9). Nutritional stress status represented the major difference in the lipid biomarkers between the two concretions possibly because the concretions were preserved under different conditions or had significantly different ages. Although no clear difference was found in the mineralogy of outer and inner concretion subsamples, except for a higher ferroan carbonate content in the outer parts, there was evidence of differences in the respective microbial communities. Both concretions had increased proportions of ω5 monounsaturates in the outer subsamples (Fig. 7) and increased markers for SRB (i17:1ω7c and 10Me16:0) in the inner subsamples (Fig. 8). This similarity suggests a variation in the microbial community during concretion formation. This variation could be related to the nature of the metal fragment at the center of the concretions.

In LC, the metal fragment showed shiny native metal in the sawn section and had only minor corrosion on its surface. This metal fragment was not analyzed for chemical composition or lipids. The metal fragment in the upper marsh creek concretion was extremely corroded such that it contained only 42% iron (Fig. 3). The Fe metal core is probably an important source of iron for siderite formation in the surrounding concretion. In a previous study, Pye et al. (1990) found that many concretions in the Warham salt marsh had no visible nucleus, but artificially seeded concretions grew more rapidly with phosphor bronze or galvanized steel nuclei than with wood or aluminum.

Concretions with broadly similar textures and mineralogy have also been reported in some of the modern intertidal sediments on the west coast of the Wash, ~50 km from the study site at Warham (Al-Agha et al. 1995). As suggested by Al-Agha et al. (1995), the cathodic corrosion of metallic iron may have played an important role in supplying the reactive Fe during the initial stage of concretion formation. They proposed the following overall reaction:

$$4Fe^0 + SO_4^{2-} + 4H_2O \rightarrow 3Fe(OH)_2 + 2OH^- + FeS.$$

This is not a simple inorganic reaction; instead, it is mediated by the activity of SRB (Hamilton 1985; King and Miller 1981). The above reaction in anaerobic corrosion is achieved by the metabolic oxidation of H_2 by the SRB (e.g. by marine *Desulfovibrio*, Hardy 1983). The reaction is comparable to the way SRB preferentially utilize H_2 rather than fermentation acids to reduce Fe(III) directly. Carbon isotope data presented elsewhere (Pye et al. 1990) clearly indicated the incorporation of biogenic HCO_3^- during the formation of authigenic carbonates within the concretions. Therefore, we conclude that microbial activity played a more important role in the cementation process than did simple cathodic corrosion of the metallic iron core.

Lipid biomarker data show a possible effect of the nature of the nucleating object. The corroded core in UC had the lowest PLFA : ResFA ratio of any concretion subsample, indicating greater cell death and accumulation of ResFA (Fig. 6), and it exhibited a high degree of stress, similar to that of the lower marsh sediment and concretion samples (Fig. 9). Moreover, the relative proportion of SRB *Desulfobulbus* (17:1ω6 in Fig. 8) was greater than that of the other two kinds of SRB. It is possible that the actively corroding metal fragment in UC developed a microbial community, dominated by *Desulfobulbus*, that could benefit from the corrosion process or products. The increase in microbially available iron would in turn drive concretion formation, in which *Desulfovibrio* would play an important role. In this model, the relatively uncorroded metal fragment in LC seems to have been a passive nucleus for concretion formation.

Conclusion

The purposes of this study were to validate the parallel application of mineralogical, geochemical, and lipid biomarker methods to sedimentary siderite concretions and their host sediments and to extend earlier observations on this system. Although spatial resolution of the concretion subsampling was limited by sample size requirements, we were able to detect differences within the concretions. Geochemical and microbial differences were found between host mud and concretion, between concretions, and between outer and inner subsamples of concretions. That most of the authigenic iron was in the form of siderite and iron oxide cements rather than sulfides strongly suggests a unique diagenetic process of aggregation and enrichment of reactive iron within the concretions against a background of bacterial sulfate reduction.

The host sediment had higher total viable biomass per gram dry weight than did its associated concretion. ResFA and the ResFA : PLFA ratio increased with depth in the sediment column and toward the center of the concretions. The great differences in microbial biomarkers between host sediments and concretions indicated the distinctive changes during the concretion formation. As the concretion grew outward by cementing host sediment particles, micro-eucaryotes, indicated by polyenoic and ω9 PLFA, were mostly excluded from the occupied pore volume. Under nutritional stress, the microbial community changed to cope with the particular environment within the concretion by transforming *cis*-monounsaturated PLFA to cyclopropyl (favored in sediments) and to *trans*-monounsaturated PLFA. The predominant SRB were more abundant in concretions than in host sediments and also varied greatly in each part of the concretions. The biomarker i17:1ω7c for *Desulfovibrio*, which is capable of reducing iron directly, was enriched within concretion subsamples, except for the corroded iron core, which had the greatest proportion of the *Desulfobulbus* biomarker 17:1ω6. Differences in microbial characteristics between the two concretions could possibly be related to different

preservation conditions in the host sediments and are most likely indicative of different formation stages. Further studies of the geochemistry and microbial ecology of this sedimentary system, in parallel with studies of pure cultures of naturally occurring iron-reducing bacteria (currently in progress), should provide a better definition of the chemical steps and organisms responsible for concretion formation.

References

AL-AGHA, M. R., S. D. BURLEY, C. D. CURTIS, AND J. ESSON. 1995. Complex cementation textures and authigenic mineral assemblages in Recent concretions from the Lincoln shire Wash (east coast, UK) driven by Fe(0) to Fe(II) oxidation. J. Geol. Soc. Lond. **152:** 157–171.

ALLISON, P. A., AND K. PYE. 1994. Early diagenetic mineralization and fossil preservation in modern carbonate concretions. Palaios **9:** 561–575.

BALKWILL, D. L., F. R. LEACH, J. T. WILSON, J. F. MCNABB, AND D. C. WHITE. 1988. Equivalence of microbial biomass measures based on membrane lipid and cell wall components, adenosine triphosphate, and direct counts in subsurface sediments. Microb. Ecol. **16:** 73–84.

BERNER, R. A. 1985. Sulphate reduction, organic matter decomposition and pyrite formation. Phil. Trans. R. Soc. Lond. Ser. A **315:** 25–38.

BLIGH, E. G., AND W. J. DYER. 1959. A rapid method of total lipid extraction and purification. Can. J. Biochem. Phys. **37:** 911–917.

CANFIELD, D. E., AND R. RAISWELL. 1991. Carbonate preservation in modern sediments, p. 337–387. *In* P. A. Allison, and D. G. Briggs [eds.], Taphonomy: Releasing the information locked in the fossil record. Plenum.

———, ———, J. T. WESTRICH, C. M.. REAVES, AND R. A. BERNER. 1986. The use of chromium reduction in the analysis of reduced inorganic sulphur in sediment and shales. Chem. Geol. **16:** 59–62.

COLEMAN, M. L. 1985. Geochemistry of diagenetic non-silicate minerals: Kinetic considerations. Phil. Trans. R. Soc. Lond. Ser. A **315:** 39–56.

———, D. B. HEDRICK, D. R. LOVLEY, D. C. WHITE, AND K. PYE. 1993. Reduction of Fe III in sediments by sulfate-reducing bacteria. Nature **361:** 436–438.

CORNWELL, J. C., AND J. W. MORSE. 1987. The characterization of iron sulphide minerals in anoxic marine sediments. Mar. Chem. **22:** 193–206.

CURTIS, C. D. 1983. Microorganisms and diagenesis of sediments, p. 263–286. *In* W. E. Krumbein [ed.], Microbial geochemistry. Blackwell.

DOWLING, N. J. E., F. WIDDEL, AND D. C. WHITE. 1986. Phospholipid ester-linked fatty acid biomarkers of acetate-oxidizing sulphate-reducers and other sulphide-forming bacteria. J. Gen. Microbiol. **132:** 1815–1825.

EDLUND, A., P. D. NICHOLS, R. ROFFEY, AND D. C. WHITE. 1985. Extractable and lipopolysaccharide fatty acid and hydroxy acid profiles from *Desulfovibrio* species. J. Lipid Res. **26:** 982–988.

FINDLAY, R. H., AND F. C. DOBBS. 1993. Quantitative description of microbial communities using lipid analysis, p. 271–284. *In* P. F. Kemp et al. [eds.], Handbook of methods in microbial ecology. Lewis.

FROELICH, P. N., AND OTHERS. 1979. Early oxidation of organic matter in pelagic sediments of the eastern equatorial Atlantic: Suboxic diagenesis. Geochim. Cosmochim. Acta **43:** 1075–1090.

FUNNELL, B. M., AND I. PEARSON. 1989. Holocene sedimentation on the north Norfolk barrier coast in relation to relative sea level changes. J. Quat. Sci. **4:** 25–36.

GAUDETTE, H. E., W. R. FLIGHT, L. TONER, AND D. FOLGER. 1974. An inexpensive titration method for the determination of organic carbon in recent sediments. J. Sediment. Petrol. **44:** 249–253.

GUCKERT, J. B., M. A. HOOD, AND D. C. WHITE. 1986. Phospholipid ester-linked fatty acid profile changes during nutrient deprivation of *Vibrio cholerae*: Increases in the *trans/cis* ratio and proportions of cyclopropyl fatty acids. Appl. Environ. Microbiol. **52:** 794–801.

HAMILTON, W. A. 1985. Sulfate-reducing bacteria and the anaerobic corrosion. Annu. Rev. Microbiol. **39:** 197–217.

HARDY, J. A. 1983. Utilisation of cathodic hydrogen by sulfate reducing bacteria. Br. Corrosion J. **18:** 190–193.

HARVEY, H. R., R. D. FALLON, AND J. S. PATTON. 1986. The effect of organic matter and oxygen on the degradation of bacterial membrane lipids in marine sediments. Geochim. Cosmochim. Acta **50:** 805–812.

HEDRICK, D. B., J. B. GUCKERT, AND D. C. WHITE. 1991. Archaebacterial ether lipid diversity: Analysis by supercritical fluid chromatography. J. Lipid Res. **32:** 656–666.

HOWARTH, R. W. 1993. Microbial processes in salt-marsh sediments, p. 239–259. *In* T. E. Ford [ed.], Aquatic microbiology. Blackwell.

JØRGENSEN, B. B., AND F. BAK. 1991. Pathways and microbiology of thiosulfate transformations and sulfate reduction in a marine sediment (Kattegat, Denmark), Appl. Environ. Microbiol. **57:** 847–856.

KING, G. M., B. L. HOWES, AND J. W. H. DACEY. 1985. Short-term endproducts of sulfate reduction in a salt marsh: Formation of acid volatile sulfides, elemental sulfur, and pyrite. Geochim. Cosmochim. Acta **49:** 1561–1566.

KING, R. A., AND J. D. A. MILLER. 1981. Corrosion by the sulphate-reducing bacteria. Nature **233:** 491–492.

LEVENTHAL, J., AND C. TAYLOR. 1990. Comparison of methods to determine degree of pyritization. Geochim. Cosmochim. Acta **54:** 2621–2625.

LOVLEY, D. R., AND OTHERS. 1993. *Geobacter metallireducens* gen. nov. sp. nov., a microorganism capable of coupling the complete oxidation of organic compounds to the reduction of iron and other metals. Arch. Microbiol. **159:** 336–344.

PARKES, R. J., AND J. TAYLOR. 1983. The relationship between fatty acid distributions and bacterial respiratory types in contemporary marine sediments. Estuarine Coastal Shelf Sci. **16:** 173–189.

PETERSON, B. J., AND R. W. HOWARTH. 1987. Sulfur, carbon, and nitrogen isotopes used to trace organic matter flow in the salt-marsh estuaries of Sapelo Island, Georgia. Limnol. Oceanogr. **32:** 1195–1213.

POSTMA, D. 1982. Pyrite and siderite formation in brackish and freshwater swamp sediments. Am. J. Sci. **282:** 1151–1183.

PYE, K. 1984. SEM analysis of siderite cements in intertidal marsh sediments, Norfolk, England. Mar. Geol. **56:** 1–12.

———. 1992. Saltmarshes on the barrier coastaline of north Norfolk, eastern England, p. 148–178. *In* J. R. L. Allen and K. Pye [eds.], Saltmarshes—Morphodynamics, conservation and engineering significance. Cambridge.

———, M. L. COLEMAN, AND W. M. DUAN. 1997. Microbial activity and digenesis in saltmarsh sediments, north Norfolk, England, p. 119–151. *In* T. Jickells and J. E. Rae [eds.], Biogeochemistry of intertidal sediments. Cambridge.

———, J. A. D. DICKSON, N. SCHIAVON, M. L. COLEMAN, AND M. COX. 1990. Formation of siderite-Mg-calcite-iron sulphide concretions in intertidal marsh and sandflat sediments, north Norfolk, England. Sedimentology **37:** 325–343.

RINGELBERG, D. B., G. T. TOWNSEND, K. A. DEWEERD, J. M. SUFLITA, AND D. C. WHITE. 1994. Detection of the anaerobic dechlorinating microorganism *Desulfomonile tiedjei* in environmental matrices by its signature lipopolysaccharide branched-long-chain hydroxy fatty acids. FEMS (Fed. Eur. Microbial. Soci.) Microbiol. Ecol. **14:** 9–18.

RODIER, L., AND M. F. KHALIL. 1982. Fatty acids in recent sediments in the St. Lawrence estuary. Estuarine Coastal Shelf Sci. **15:** 473–483.

SKYRING, C. W. 1987. Sulfate reduction in coastal ecosystems. Geomicrobiol. J. **5:** 295–373.

TAYLOR, J., AND R. J. PARKES. 1983. The cellular fatty acids of the sulfate-reducing bacteria *Desulfobacter* sp., *Desulfobulbus* sp., and *Desulfovibrio desulfuricans*. J. Gen. Microbiol. **129:** 3303–3309.

VESTAL, J. R., AND D. C. WHITE. 1989. Lipid analysis in microbial ecology. Quantitative approaches to the study of microbial communities. BioScience **39:** 535–541.

VOLKMAN, J. K., R. B. JOHNS, F. T. GILLAN, AND G. J. PERRY. 1980 Microbial lipids of an intertidal sediment—1. Fatty acids and hydrocarbons. Geochim. Cosmochim. Acta **44:** 1133–1143.

WHITE, D. C. 1968. Lipid composition of the electron transport membrane of *Haemophilus parainfluenzae*. J. Bacteriol. **96:** 1159–1170.

———. 1993. In situ measurement of microbial biomass, community structure and nutritional status. Phil. Trans. R. Soc. Lond. Ser. A **344:** 59–67.

———, R.J. BOBBIE, J. D. KING, J. NICKELS, AND P. AMOE. 1979. Lipid analysis of sediments for microbial biomass and community structure, p. 87–103. *In* C. D. Litchfield and P. L. Seyfried [eds.], Methodology for biomass determinations and microbial activities in sediments. Am. Soc. Testing Mater. ASTM STP 673.

———, AND OTHERS. 1983. The ground water aquifer microbiota: Biomass, community structure and nutritional status. Dev. Ind. Microbiol. **24:** 201–211.

Submitted: 14 September 1995
Accepted: 6 March 1996
Amended: 2 July 1996